Assessment of CryoSat-2 interferometric and non-interferometric SAR altimetry over ice sheets

Malcolm McMillan [a,*], Andrew Shepherd [a], Alan Muir [b], Julia Gaudelli [b], Anna E. Hogg [a], Robert Cullen [c]

[a] Centre for Polar Observation and Modeling, School of Earth and Environment, University of Leeds, Leeds LS2 9JT, UK
[b] University College London, Gower Street, London WC1E 6BT, UK
[c] ESA ESTEC, Keplerlaan 1, 2201 AZ Noordwijk, The Netherlands

Abstract

The launch of CryoSat-2 heralded a new era of interferometric Synthetic Aperture Radar altimetry over the Polar Ice Sheets. The mission's novel SAR interferometric (SARIn) mode of operation has enabled monitoring of rapidly changing coastal regions, which had been challenging for previous low resolution altimeters. Given the growing requirement to continue the 25-year altimeter record, there is now a need to assess the differences between existing SAR and SARIn altimeter datasets, with a view to understanding the impact on ice sheet retrievals of the different radar hardware and processing methodologies. Uniquely, CryoSat-2 data can be processed both with and without interferometric information, offering the opportunity to directly compare the SAR and SARIn products generated by the current ground segment. Here, we provide a first comparison of these Level-2 datasets, and evaluate their capacity to measure ice sheet elevation and elevation change. We find that the current interferometric product has substantially improved precision, accuracy and coverage compared to its non-interferometric counterpart, yielding a ~35% improvement in the root-mean-square-difference (RMSD) of elevations recorded at orbital cross-overs, and a ~30% lower RMSD of elevation rates relative to Operation IceBridge airborne altimeter measurements. This analysis demonstrates the value that the interferometer adds to the current CryoSat-2 configuration, and highlights the importance for non-interferometric SAR Level-2 processing of the auxiliary data used to identify the location of the echoing point. These results provide a benchmark of the relative performance of the Level-2 interferometric and non-interferometric products currently produced by the ground segment, which will help to inform the design and implementation of a future polar radar altimeter mission.
© 2017 COSPAR. Published by Elsevier Ltd. This is an open access article under the CC BY license (http://creativecommons.org/licenses/by/4.0/).

1. Introduction

For the past quarter of a century, satellite radar altimeters have acquired measurements across Earth's polar regions, mapping the ice sheets of Greenland and Antarctica at the continental scale, and establishing a near continuous record of ice sheet elevation evolution. These observations have provided systematic measurements of changes in ice sheet volume (Davis and Ferguson, 2004; Johannessen et al., 2005; Helm et al., 2014) and mass (Wingham et al., 2006b; Zwally et al., 2011; Shepherd et al., 2012; McMillan et al., 2014a, 2016), which have informed community assessments of global mean sea level rise (Vaughan et al., 2013). With their capacity to resolve changes at the scale of individual glacier basins, they have

tracked signals of ice imbalance in Antarctica (Shepherd et al., 2001; Flament and Rémy, 2012; McMillan et al., 2014a; Wouters et al., 2015), Greenland (Zwally et al., 2005; Sørensen et al., 2015; McMillan et al., 2016) and the Arctic (McMillan et al., 2014b; Gray et al., 2015). They have also provided detailed topographic information (Remy et al., 1989; Bamber and Bindschadler, 1997; Bamber et al., 2009; Helm et al., 2014), which provides a boundary condition for numerical ice sheet models.

Many of these altimeter records have been derived using conventional, pulse-limited radar instruments, which were originally developed to measure the ocean geoid, and which have been routinely operated onboard the ERS-1, ERS-2 and Envisat satellites between 1991 and 2012. One of the principle challenges when using these data to measure ice sheet surfaces comes from their relatively large ground footprint, which is approximately $2 \, km^2$ (pulse-limited footprint over a flat surface). This has often limited their performance in areas of complex topographic terrain, which are typical of an ice sheet's margin. In 2010, the launch of CryoSat-2 represented the most significant recent advance in system evolution, through the implementation of interferometric synthetic aperture radar (SARIn) altimeter instrumentation and processing techniques (Raney, 1998; Wingham et al., 2006a). The novel altimeter carried by CryoSat-2 provided a 4-fold improvement in along-track ground resolution (to ∼400 m) through SAR processing, and enabled more precise echo location using its two antennas and interferometric techniques. Together with the satellite's high inclination and long repeat orbit, these advances have improved signal retrieval across areas of complex ice margin terrain (McMillan et al., 2013, 2014a).

In the seven years since launch, CryoSat-2 has delivered detailed trends in Earth's ocean and land based ice masses (Laxon et al., 2013; Helm et al., 2014; McMillan et al., 2014a, 2016; Tilling et al., 2015). Additionally over water surfaces, CryoSat-2 has been used to monitor lake and river levels (Nielsen et al., 2015; Villadsen et al., 2015), ocean surface height and dynamic topography (Armitage et al., 2016), and through inversion of the detected sea surface gradients, marine bathymetry (Sandwell et al. (2014)). Although CryoSat-2 remains in operation, the mission is now in an extended phase beyond its original design lifetime, which was 3.5 years. Given the growing requirement for continuity of measurements of Earth's polar regions, and the new generation of SAR and SAR interferometric altimeters, there is a need to establish the relative accuracies of these modes of operation, as delivered by the current ground segment. Such analysis can help to quantify the uncertainties associated with current Level-2 (L2) products, identify avenues for further methodological developments, and inform decisions related to future mission design. In this study we conduct such a comparison to assess CryoSat-2 Level-2 measurements over ice sheets, which have been derived using both interferometric and non-interferometric processing techniques.

2. Data and methods

2.1. Interferometric SAR data

For the purposes of this study, our interferometric dataset was taken from the standard L2 SARIn (SIN) product, which was derived using the nominal interferometric processor. In this mode of operation, CryoSat-2 uses delay-Doppler (SAR) processing to improve along-track ground resolution to ∼400 m (Wingham et al., 2006a; McMillan et al., 2013), and the phase difference recorded across the two antennas to determine the angle of echo arrival in the across-track plane. Given that Baseline C reprocessing was incomplete at the time of the analysis, we primarily used the Baseline B product distribution, as it provided the long, multi-year record that was required for our study. However, for short time period crossover analysis, we also evaluated several of the available sub-cycles of Baseline C data, to assess the relative performance of the two baselines. For ice sheet studies, Baseline C implements a number of relevant changes, including (1) stack weighting, which removes beams with the largest look angle so as to improve the signal-to-clutter noise ratio, (2) a refined DEM, which is expected to reduce the number of SARIn records flagged as being in error, and (3) an increase in the range window of the SARIn product, from 120 m to 240 m, which reduces the instances where waveform truncation adversely affects the retracking process.

2.2. Non-interferometric SAR data and processing

To generate a non-interferometric SAR L2 product over ice sheets, we utilized the non-operational SARIn Degraded (SID) processor option. This option originated from CryoSat-1, where the altimeter radar hardware was designed as a single, non-redundant, instrument, and so contingency was needed for a scenario in which one of the two receive chains failed. In case of such failure, the radar was designed to still operate in this degraded case and therefore an on-ground processing capability was needed. This scenario was termed SARIn Degraded Mode (SID) and the processing method combined existing SARIn and Low Resolution Mode (LRM) functionality.

The SARIn Degraded processing that was implemented in this study used only one of the SARIn chains, which was chosen to be the rx-1 chain. The functionality was otherwise similar to the nominal processing to Level-1b, although the Level-1b interferometric phase difference and coherence were not filled in the product. The Level-2 SID processing then followed closely to that of LRM, with the exception that the LRM retracker was replaced by the nominal SARIn retracker (Wingham et al., 2006a). Following retracking, the echoing point was relocated to the point of closest approach using the slope model that is implemented in the most recent Baseline C version of the ESA L2 processors, which is derived from the Radarsat Antarctic Mapping Project (RAMP) version 2 Digital Elevation

Model (Liu et al., 2015). This model was chosen in accordance with the objectives of this work, which were to evaluate the performance of existing Level-2 products, as generated by the processing implemented in the current ground segment. For records where the slope model was unavailable, the data were flagged and the echoing point was assumed to be at nadir.

2.3. Evaluation of elevation precision

The precision of the SIN and SID elevation measurements was assessed using a single sub-cycle crossover technique (Wingham et al., 1998). For data acquired in each 30-day sub-cycle, all crossing points within the grounded ice region of the CryoSat-2 SARIn mode mask were identified. Specifically, crossing points were defined as the intersection between two consecutive measurements of an ascending pass and two consecutive measurements of a descending pass. The elevation difference (dH) between ascending and descending acquisitions was then computed by interpolating the bracketing ascending and descending records to the crossover location. To avoid dH estimates where there was low confidence in either the accuracy of the contributing measurements or the along-track interpolation, we removed crossovers where the magnitude of dH between ascending and descending acquisitions exceeded 10 meters, or where the interpolated records were further than 1 km from each other.

2.4. Estimation of rates of elevation change

We estimated rates of ice sheet surface elevation change using a model-fit method (McMillan et al., 2014a). In comparison to a conventional cross-over approach (Wingham et al., 1998), this method extends retrievals beyond the locations of orbit cross-overs to include all data acquired along the satellite track (Pritchard et al., 2009; Smith et al., 2009; Moholdt et al., 2010; Flament and Rémy, 2012; McMillan et al., 2014a). This approach allows a far greater volume of data to be utilized and is particularly well-suited to the long 369-day orbit cycle of CryoSat-2, where exact repeats are less frequent. We grouped data in 5×5 km regions and the elevations within each grid cell were modeled as a function of space, time and satellite heading (McMillan et al., 2014a). Based on previous studies where we found that valid data were often unnecessarily flagged within the L2 product, our method was designed instead to use all SID and SIN data, and then to apply an iterative approach within our elevation change derivation to identify and remove bad data (McMillan et al., 2014a, 2016). Given the novelty of the SID product, however, we did also process an additional scenario where all flagged SID data were removed. Following previous studies that have utilized CryoSat-2 SARIn data over Antarctica (McMillan et al., 2014a; Konrad et al., 2016), a backscatter correction was applied to account for temporally correlated fluctuations in elevation and backscatter

(Wingham et al., 1998; Davis and Ferguson, 2004). Grid cells where the model was a poor fit to the data were rejected, and estimates of the linear rate of elevation change with time were extracted for each grid cell, together with regression statistics, which described the associated precision and model goodness of fit. Elevation rates were then smoothed with a 25×25 km moving median filter for display purposes. Further details relating to the method and model implementation are given in McMillan et al. (2014a; 2016).

2.5. Evaluation using auxiliary datasets

To evaluate our derived rates of elevation change, we used elevation measurements acquired by the Airborne Topographic Mapper (ATM) laser altimeter on Operation IceBridge campaigns flown between 2009 and 2013. This instrument provides surface elevation measurements, sampled approximately 50 m along track, with a fixed 80 m across-track platelet at aircraft nadir. The ATM elevation measurements are estimated to have a vertical accuracy of 7 cm and a vertical precision of 3 cm (Martin et al., 2012). We selected a validation site in the Amundsen Sea Sector of West Antarctica, which offers (1) a high density of airborne flightlines, (2) acquisitions made over multiple years which can be used to compute elevation change, and (3) a large range of elevation rate variability.

To compute rates of elevation change from repeat Ice-Bridge measurements of surface elevation, we differenced ATM observations that were co-located to within 10 meters horizontal separation. We then scaled the elevation difference in accordance with the time separation between the measurements to derive an estimate of the annual rate of change. Elevation change rates with a magnitude greater than 10 m/yr were removed, and the remaining measurements were then binned at 5 km resolution to match the CryoSat-2 estimates. Grid cells sampled by fewer than 10 IceBridge elevation change measurements, or where the measurements had a standard deviation greater than 1 m/yr were removed. These thresholds were applied in order to ensure a robust set of observations with which to evaluate our CryoSat-2 datasets.

3. Results

3.1. Evaluation of elevation measurements

As a first, qualitative comparison of the SIN and SID Level-2 elevation measurements, we investigated their ability to map ice surface topography at a test site with relatively complex surface topography. For this purpose, we chose a site in East Antarctica above the drained Cook E2 subglacial lake, where a large surface depression is known to have formed (Smith et al., 2009; McMillan et al., 2013). We used ~1 cycle of SIN and SID elevation data to each generate a surface elevation model, by fitting a minimum curvature surface (Sandwell, 1987) to each

dataset. For the SID measurements, we tested two scenarios, one in which flagged data were included and the other in which they were removed.

The elevation models produced from the SIN and SID measurements (Fig. 1) illustrate the differing capabilities of each mode to resolve 10-km length-scale features in the ice sheet surface. The SIN measurements provided a detailed view of the surface depression, because the interferometer was able to track the across-track angle of echo arrival. Consequently it has been able to correctly locate the origin of the strongest power return, which switched between the rim and the base of the depression. In contrast,
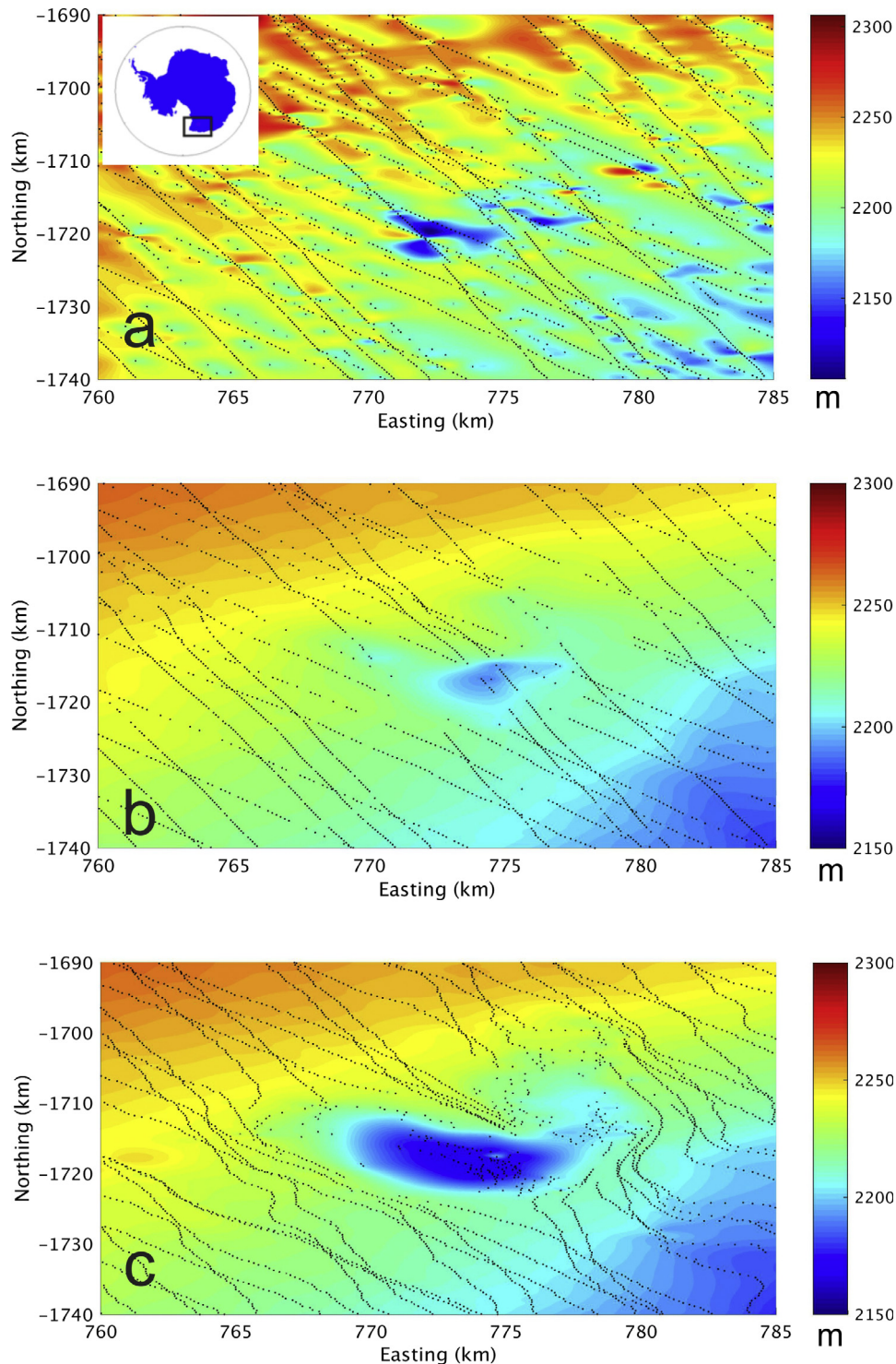

Fig. 1. Comparison of the capability of CryoSat-2 interferometric and non-interferometric Level-2 data to resolve ice sheet surface topography above the CookE2 subglacial lake in East Antarctica. In each panel a continuous elevation model has been formed by interpolating CryoSat-2 measurements acquired during 2011, with the echoing point locations shown in black. a. all SIN data; b. all SID data; c. flagged SID data removed.

both SID solutions failed to resolve the true shape and depth of this feature because the increase in range cannot be associated with a change in the angle of arrival, due to limitations in the surface slope model used in the non-interferometric L2 processing. Comparing the two SID solutions, it is clear that the inclusion of flagged data in the elevation model added more high frequency noise to the solution. This is because, in contrast to when we determine elevation change, no independent quality control procedure was used to identify and remove bad elevation data. Further analysis relating to the impact of removing flagged data on the derived rates of elevation change is given in the Discussion section.

Next, we assessed the repeatability of SIN and SID elevation measurements, using a single-cycle crossover technique (Wingham et al., 1998). Elevation residuals at crossovers broadly indicate the precision of the elevation retrieval, and integrate a number of factors, including spatially uncorrelated orbit errors, retracker imprecision, radar speckle, echo relocation errors and any sensitivity to anisotropic scattering in the near surface snowpack. In comparison to non-interferometric measurements, where only a single crossover is resolved at each ground track intersection, the capability of the interferometer to resolve high frequency variability in the echoing point location allows for the possibility of multiple crossing points to be identified at a single ground track intersection. Based on the analysis of two sub-cycles of Baseline B data and two sub-cycles of Baseline C data (Table 1), SIN outperforms the SID processing, delivering a smaller median crossover elevation difference (−0.006 m and 0.055 m for SIN and SID, respectively, statistically significant difference at the 5% level) and less dispersion of the differences (standard deviations of 2.7 m and 3.3 m for SIN and SID respectively). The improved performance of SIN is evident from the distributions of elevation differences for the different processing scenarios (Fig. 2), specifically relative to Baseline C, which due to the increased number of crossovers returned for SID, offers a closer like-for-like comparison to SIN (Table 1). Although for Baseline B the dH statistics for SIN and SID are more similar, SIN achieves ∼7 times the number of cross-overs returned by SID, demonstrating the superior density of measurements offered by the SIN mode of operation.

3.2. Evaluation of rates of elevation change

Using our SIN and SID datasets, we estimated linear rates of elevation change between 2011 and 2014 (Fig. 3). Taking the whole of the Antarctic margin region covered by the CryoSat-2 interferometric mode mask, the SID elevation rate measurements provide less complete coverage, with 16% of grid cells lacking a valid elevation rate measurement, compared to 11% for the SIN dataset. The loss of data in the SID result is particularly apparent across the Antarctic Peninsula and Transantarctic Mountains, highlighting the value of interferometric altimetry in locat-

Table 1
SIN and SID crossover statistics for Baseline-B and Baseline-C sub-cycles. Note that the SID statistics for Baseline-B are based on far fewer cross-overs than for Baseline-C, indicating the poorer coverage of cross-overs achieved by the earlier baseline.

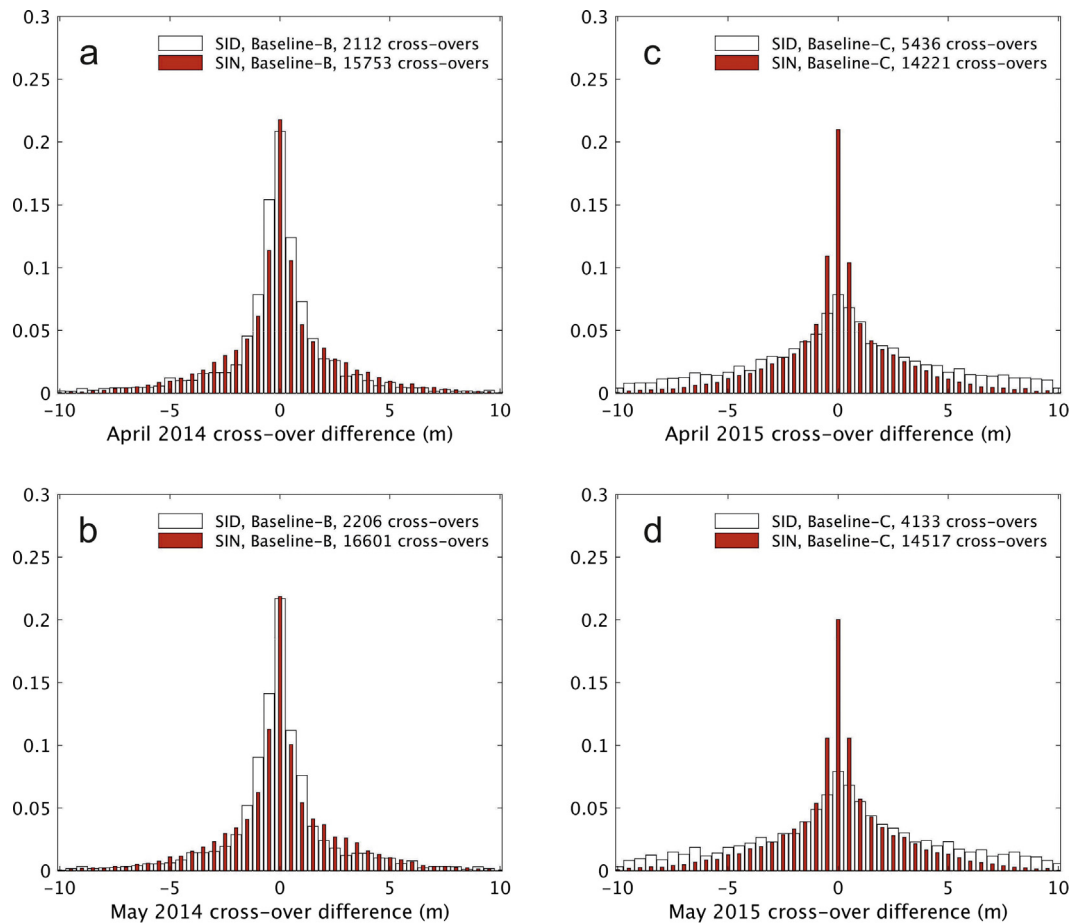|	Number of cross-overs		Mean cross-over height difference (m)		Median cross-over height difference (m)		Standard deviation of cross-over height differences (m)		Root-mean-square of cross-over height differences (m)	
	SIN	SID	SIN	SID	SIN	SID	SIN	SID	SIN	SID
Baseline B, cycle 1	15,753	2112	−0.006	−0.13	−0.02	−0.03	2.61	2.44	2.61	2.45
Baseline B, cycle 2	16,601	2206	0.03	−0.04	−0.01	−0.07	2.64	2.45	2.64	2.45
Baseline C, cycle 1	14,221	5436	0.02	0.18	0.002	0.15	2.77	4.22	2.77	4.22
Baseline C, cycle 2	14,517	4133	0.01	0.16	0.006	0.16	2.84	4.28	2.84	4.28
Mean	15,273	3472	0.01	0.04	−0.006	0.05	2.71	3.35	2.71	3.35

Fig. 2. Comparisons of normalised distributions of SID and SIN crossover height differences, for Baseline B data acquired during two sub-cycles in **a.** April and **b.** May 2014 and Baseline C data acquired during two sub-cycles in **c.** April and **d.** May 2015. SIN returns a greater number of crossovers and, for Baseline C, exhibits much less dispersion of the crossover differences. SID crossover differences appear less dispersed for Baseline B because far fewer crossovers are returned than for Baseline C.

ing the echo in regions of complex topographic terrain (Fig. 3).

Both SIN and SID resolve high rates of ice sheet thinning in the Amundsen Sea and Bellingshausen Sea Sectors of West Antarctica, and close to the terminus of Totten Glacier in East Antarctica (Fig. 3). However, around much of the remainder of the ice sheet, particularly in slower flowing, inland regions, the SID data produce relatively high rates of elevation change that are not associated with known geophysical signals (Pritchard et al., 2009; Flament and Rémy, 2012; Shepherd et al., 2012; Helm et al., 2014; McMillan et al., 2014a). We interpret this to be indicative of increased levels of noise in the non-interferometric solution, which is supported by the diagnostic statistics associated with the elevation rate precision (Fig. 3). In this regard, SIN outperforms SID, achieving a mean statistical uncertainty of 0.18 m/yr, compared to 0.67 m/yr for the SID dataset.

To provide an independent evaluation of the SIN and SID elevation rates, we then compared both datasets to co-located IceBridge measurements across the Amundsen Sea Sector of West Antarctica (Fig. 4). Although the average difference is actually smaller for SID than for SIN (Table 2), the dispersion of the SID differences is ~50% greater, and the correlation with IceBridge elevation rates is significantly (at the 1% significance level) weaker for SID than it is for SIN (Pearson correlation coefficients of 0.50 and 0.70, respectively). Together, these statistics indicate the poorer agreement of the individual SID elevation rates with the IceBridge reference dataset. This is reflected in the root mean square deviation of the SIN and SID measurements from the IceBridge data, which is 1.11 m/yr and 1.66 m/yr, respectively (Table 2).

4. Discussion

In this study we have aimed to provide a first assessment of the relative performance of interferometric and non-interferometric CryoSat-2 Level 2 SAR altimetry products over ice sheets, as generated by the current ground segment. Specifically, we have focused on the accuracy and precision of retrievals of ice sheet elevation and elevation change. These are important glaciological parameters that
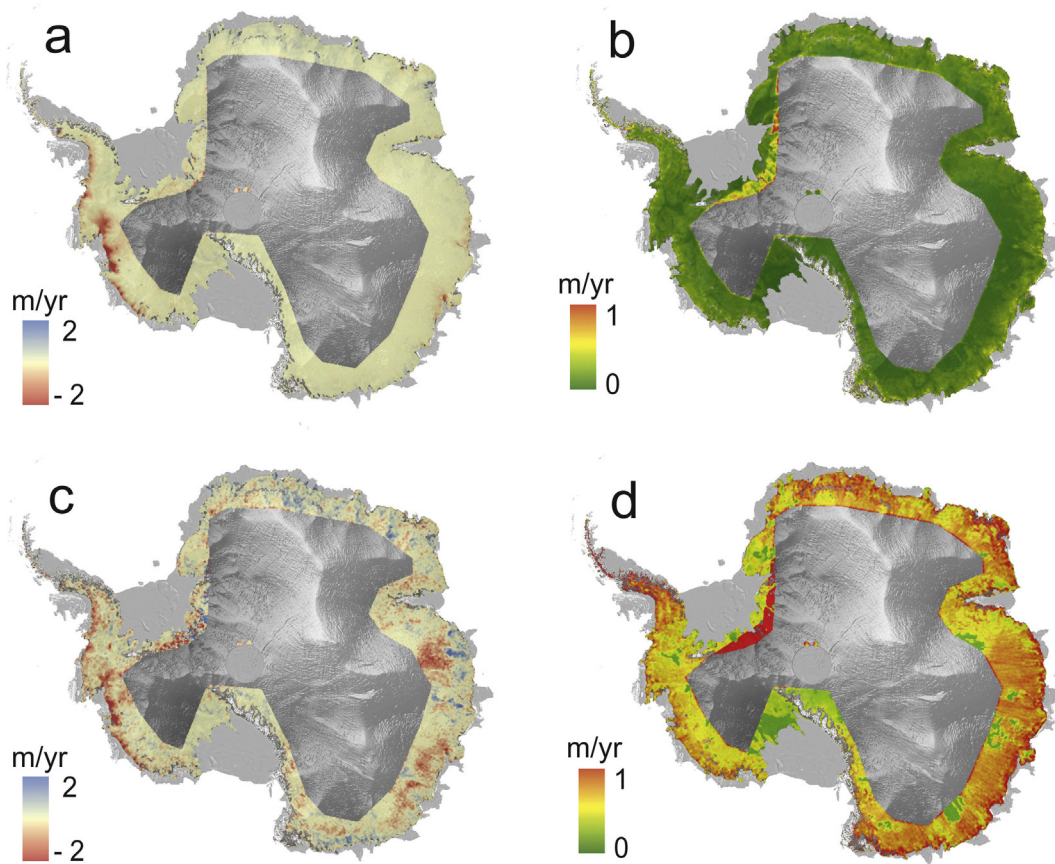
Fig. 3. Comparison of rates of Antarctic Ice Sheet elevation change estimated using a model fit method for data acquired between 2011 and 2014, and which were derived from **a.** SIN and **c.** SID datasets, together with the 67% confidence interval associated with the **b.** SIN and **d.** SID elevation rates. Results are determined across the ice margin region covered by the SARIn mode mask.
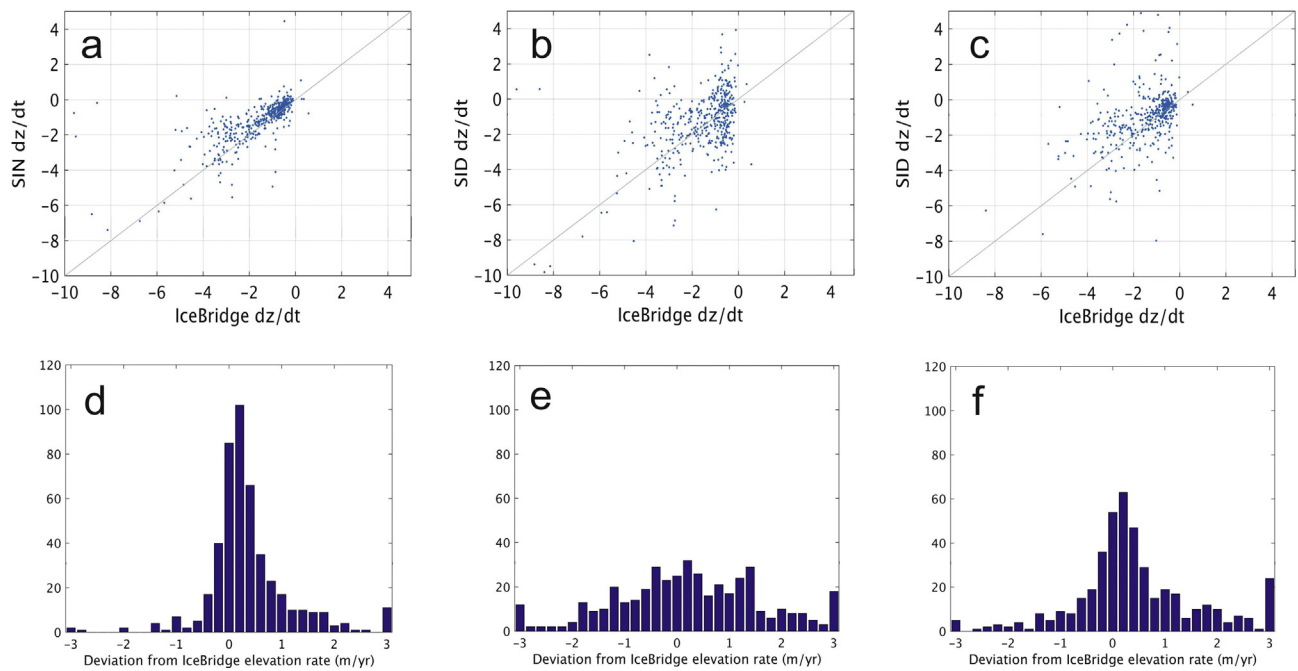

Fig. 4. Comparison of rates of surface elevation change derived from CryoSat-2 with those from co-located IceBridge airborne altimetry data across the Amundsen Sea Sector of West Antarctica. CryoSat-2 elevation rates are derived using **a.** SIN data, **b.** all SID data, and **c.** SID data with flagged records removed. Panels **d-f** show the corresponding distributions of the differences between the CryoSat-2 and IceBridge elevation rate measurements.

Table 2
Summary statistics for the comparison to IceBridge airborne altimetry of elevation rates derived from SIN data, all SID data, and SID data with flags removed.

| Statistic	SIN	SID	SID flags removed
Mean difference from IceBridge elevation rates	0.40 m/yr	0.26 m/yr	0.51 m/yr
Median difference from IceBridge elevation rates	0.24 m/yr	0.20 m/yr	0.25 m/yr
Standard deviation of the differences from IceBridge elevation rates	1.03 m/yr	1.64 m/yr	1.55 m/yr
Root-mean-square difference from IceBridge elevation rates	1.11 m/yr	1.66 m/yr	1.63 m/yr
Pearson correlation coefficient	0.70	0.50	0.41
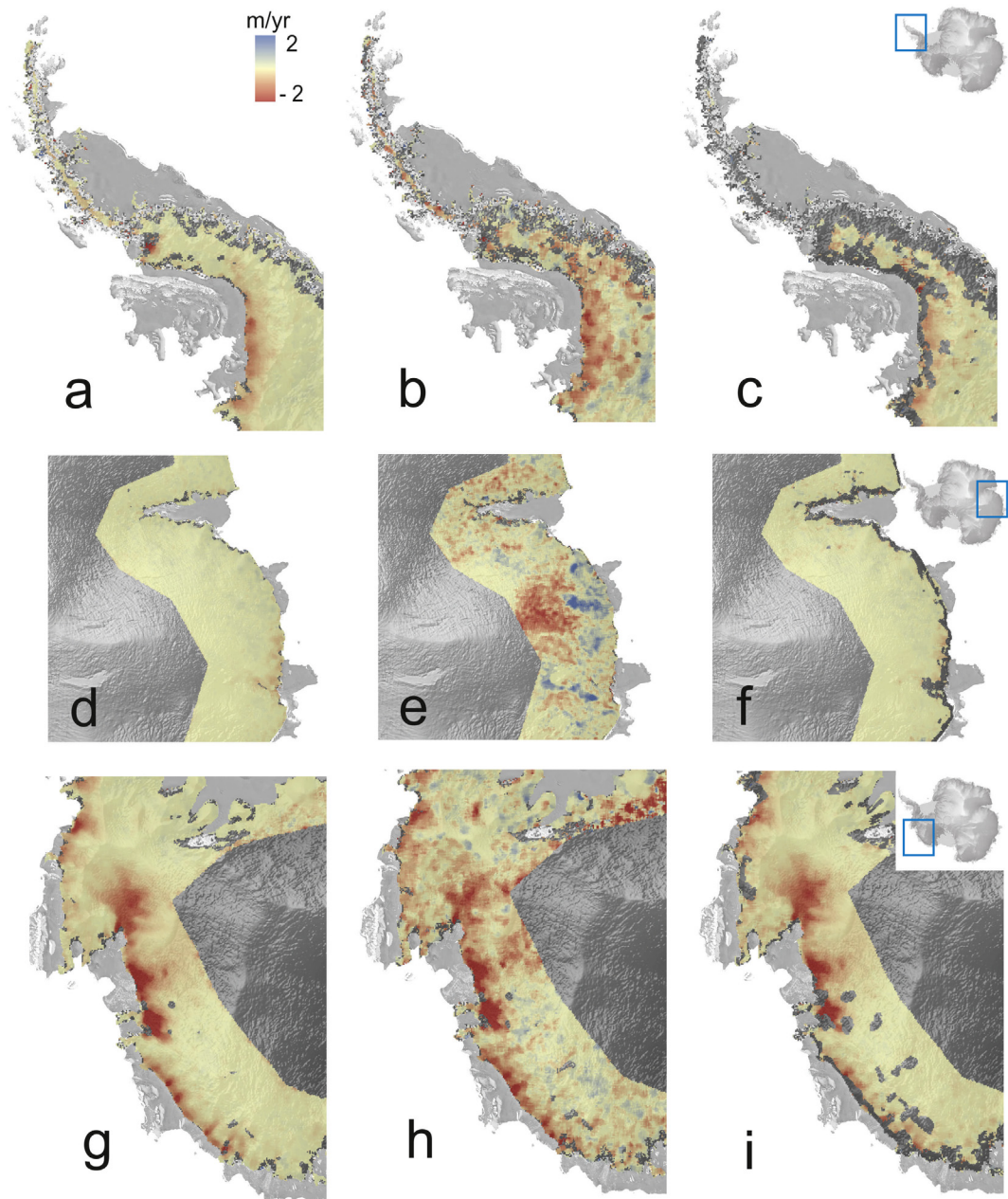
Fig. 5. Comparison of elevation rates derived from SIN and SID data in coastal areas with more complex topography. **a-c.** the Antarctic Peninsula; **d-f.** the Indian Ocean Sector of East Antarctica; **g-i.** the Amundsen Sea Sector of West Antarctica; **a, d, g.** using SIN data; **b, e, h.** using all SID data; **c, f, j.** using SID data with flagged records removed. The solution derived using all SID data provides comprehensive coverage but displays a relatively noisy signal, whereas removal of flagged SID data gives a less noisy signal, particularly in inland regions, but fails to retrieve much of the rapid coastal thinning. In contrast SIN data provides both low noise and near-complete coverage of the coastal regions.

are used to determine systematic, long-term records of ice sheet mass balance and sea level contribution.

As outlined in our methods, based on past analysis (McMillan et al., 2014a) we chose to use all SID and SIN measurements in our elevation rate processing, in order to maximize data coverage and avoid removing mistakenly flagged records. To test this approach, we additionally ran a scenario where we simply removed all flagged SID data prior to computing rates of elevation change. We found that, while this approach led to more precise signal retrieval in some regions and a visually less noisy solution, it had a substantial impact on coverage, with 24% of grid cells within the SARIn mode mask failing to return a valid elevation rate measurement. Furthermore, coverage was particularly reduced around most of the steeper ice sheet margin (Fig. 5), which is amongst the most important area to monitor, given that this is where current rates of ice loss are at their greatest. Although removing flagged data did improve the mean precision of elevation rate retrievals to 0.31 m/yr, this is in part because of the more restricted spatial coverage and, nonetheless, it still remained approximately double the SIN value (0.18 m/yr). In addition, there was almost no difference between the two SID processing scenarios in terms of their agreement with the Ice-Bridge reference datasets (RMS differences of 1.63 m/yr and 1.66 m/yr, and correlation coefficients of 0.41 and 0.50, when flagged data were, and were not, removed). As such, while this analysis suggests that there is a payoff between the spatial coverage and measurement precision achieved by the two non-interferometric processing scenarios, it is clear that neither of these SID datasets currently matches the performance of the SIN observations.

This study was designed to assess the current performance of existing SIN and SID processing baselines. Based upon these results, we can therefore make the following recommendations and suggestions for future work. Firstly, while we find that non-interferometric retrievals cannot currently match the quality of their interferometric counterparts, our analysis does highlight the importance, for the former, of the accuracy of the slope model used to relocate the echoing points. To optimize the performance and coverage achieved by non-interferometric SAR altimeters, and potentially improve upon the SID results reported here, it is important that future SAR L2 processors (1) utilize the latest, most accurate DEM products when relocating the echo, and (2) have well-tuned flagging mechanisms. Secondly, this study was designed to inter-compare L2 SIN and SID measurements derived from the same data acquisitions, so as to achieve a contemporaneous like-for-like comparison, which eliminated differences due to temporal variability and isolated the value of the interferometer itself. As a consequence, it is worth emphasizing that this study does not represent an evaluation of the performance of SIN (CryoSat-2) relative to other SAR (Sentinel-3) altimeters. Such an analysis is therefore recommended as part of future work, albeit over the different time periods during which the missions have operated. This would provide a complementary assessment, which in addition to comparing SAR and SARIn acquisitions, would also address the impact of other differences between the Cryosat-2 and Sentinel-3 missions, namely (1) the orbital inclination and repeat period, (2) the range dimensions of the receive window, (3) the number of bursts per unit time, to assess the optimal effective number of looks for land ice surfaces, and (4) the design of onboard surface tracking algorithms. Finally, it is worth reiterating that here we have focused on inter-comparing existing L2 data. Clearly there are also other benefits to an interferometric system, such as the improved data density that can be achieved by utilizing swath processing (Hawley et al., 2009; Gray et al., 2013).

5. Conclusions

This study has provided a first comparison between CryoSat-2 interferometric and non-interferometric altimeter Level-2 products over ice sheets, and an indication of the benefits associated with the former. Regarding measurements of ice sheet elevation, we firstly demonstrated that currently the interferometric retrievals are able to better map small-scale topographic features, such as the surface manifestation of subglacial lakes. Systematic mapping of these features can provide valuable insight into the nature and evolution of the inaccessible subglacial environment (Smith et al., 2009), which improves our understanding of the underlying boundary conditions of the ice sheet, and benefits physical models of ice sheet evolution. Secondly, we find that the interferometric processing offered more precise elevation measurements across the ice sheet margins, achieving a ~35% reduction in the Root-Mean-Square Difference of single-cycle cross-overs formed from 2 sub-cycles of Baseline C data. In this regard, improved elevation precision benefits topographic mapping, assessments of snowpack anisotropy (Remy et al., 2012; Armitage et al., 2014) and altimeter-derived time series of surface elevation change (Wingham et al., 2009).

For measuring ice sheet surface elevation change, we find that the current generation of interferometric measurements is in closer agreement to independent airborne observations than their non-interferometric counterparts. Specifically, SIN measurements achieve a ~30% reduction in the Root-Mean-Square deviation and improvements in the correlation coefficient from 0.50 (SID) to 0.70 (SIN), relative to this reference dataset. These results suggest that, using current processing baselines, SIN measurements are able to more accurately resolve signals of elevation change. We also find that CryoSat-2 SIN observations yield at least a ~2-fold improvement in the mean precision of elevation rates, together with more complete spatial coverage, which again indicates the benefits offered currently by the interferometric system. In a wider context, determining rates of elevation change with a high level of accuracy is critical for building robust records of ice sheet mass balance and sea level rise. The results of this study suggest that the interferometric CryoSat-2 product is demonstrably better

able to achieve this at present, and indicates the potential value of an interferometer onboard a future polar altimeter mission.

Acknowledgements

References

Armitage, T.W.K., Wingham, D.J., Ridout, A.L., 2014. Meteorological origin of the static crossover pattern present in low-resolution-mode cryoSat-2 data over central antarctica. IEEE Geosci. Remote Sens. Lett. 11 (7), 1295–1299. https://doi.org/10.1109/LGRS.2013.2292821.

Armitage, T.W.K., Bacon, S., Ridout, A.L., Thomas, S.F., Aksenov, Y., Wingham, D.J., 2016. Arctic sea surface height variability and change from satellite radar altimetry and GRACE, 2003–2014. J. Geophys. Res. Ocean. 121 (6), 4303–4322. https://doi.org/10.1002/2015JC011579.

Bamber, J.L., and R. A. Bindschadler (1997), An improved elevation dataset for climate and ice-sheet modelling: validation with satellite imagery, edited by J. E. Walsh, Ann. Glaciol., 25, 438–444.

Bamber, J.L., Gomez-Dans, J.L., Griggs, J.A., 2009. A new 1 km digital elevation model of the Antarctic derived from combined satellite radar and laser data - Part 1: Data and methods. Cryosph. 3 (1), 101–111.

Davis, C., Ferguson, A., 2004. Elevation change of the Antarctic ice sheet, 1995–2000, from ERS-2 satellite radar altimetry. IEEE Trans. Geosci. Remote Sens. 42 (11), 2437–2445. https://doi.org/10.1109/TGRS.2004.836789.

Flament, T., Rémy, F., 2012. Dynamic thinning of Antarctic glaciers from along-track repeat radar altimetry. J. Glaciol. 58 (211), 830–840. https://doi.org/10.3189/2012JoG11J118.

Gray, L., Burgess, D., Copland, L., Cullen, R., Galin, N., Hawley, R., Helm, V., 2013. Interferometric swath processing of Cryosat data for glacial ice topography. Cryosph. 7 (6), 1857–1867. https://doi.org/10.5194/tc-7-1857-2013.

Gray, L., Burgess, D., Copland, L., Demuth, M.N., Dunse, T., Langley, K., Schuler, T.V., 2015. CryoSat-2 delivers monthly and inter-annual surface elevation change for Arctic ice caps. Cryosph. Discuss. 9 (3), 2821–2865. https://doi.org/10.5194/tcd-9-2821-2015.

Hawley, R.L., Shepherd, A., Cullen, R., Helm, V., Wingham, D.J., 2009. Ice-sheet elevations from across-track processing of airborne interferometric radar altimetry. Geophys. Res. Lett. 36 (22), L22501. https://doi.org/10.1029/2009GL040416.

Helm, V., Humbert, A., Miller, H., 2014. Elevation and elevation change of Greenland and Antarctica derived from CryoSat-2. Cryosph. 8 (4), 1539–1559. https://doi.org/10.5194/tc-8-1539-2014.

Johannessen, O.M., K. Khvorostovsky, M. W. Miles, and L. P. Bobylev (2005), Recent ice-sheet growth in the interior of Greenland., Science 310 (5750), 1013–1016, doi:10.1126/science.1115356.

Konrad, H., Gilbert, L., Cornford, S.L., Payne, A., Hogg, A., Muir, A., Shepherd, A., 2016. Uneven onset and pace of ice-dynamical imbalance in the Amundsen Sea Embayment, West Antarctica. Geophys. Res. Lett. 43, 910–918. https://doi.org/10.1002/2016GL070733.

Laxon, S.W., Giles, K.A., Ridout, A.L., et al., 2013. CryoSat-2 estimates of Arctic sea ice thickness and volume. Geophys. Res. Lett. 40 (4), 732–737. https://doi.org/10.1002/grl.50193.

Liu, H., Jezek, K.C., Li, B., Zhao, Z., 2015. Radarsat Antarctic Mapping Project Digital Elevation Model, Version 2, Boulder. NASA National Snow and Ice Data Center Distributed Active Archive Center, Colorado USA.

Martin, C.F., W.B., Krabill, S.S., Manizade, R.L., Russell, J.G., Sonntag, R.N., Swift, and J. K., Yungel (2012), Airborne Topographic Mapper Calibration Procedures and Accuracy Assessment, NASA Tech. Rep. NASA/TM-2012-215891, Goddard Sp. Flight Center, Greenbelt, Maryl. 20771. Available online http://ntrs.nasa.gov/archive/nasa/casi.ntrs.nasa.gov/20120008479.pdf.

McMillan, M., Corr, H., Shepherd, A., Ridout, A., Laxon, S., Cullen, R., 2013. Three-dimensional mapping by CryoSat-2 of subglacial lake volume changes. Geophys. Res. Lett. 40 (16), 4321–4327. https://doi.org/10.1002/grl.50689.

McMillan, M., Shepherd, A., Sundal, A., Briggs, K., Muir, A., Ridout, A., Hogg, A., Wingham, D., 2014a. Increased ice losses from Antarctica detected by CryoSat-2. Geophys. Res. Lett. 41, 3899–3905. https://doi.org/10.1002/2014GL060111.

McMillan, M., Shepherd, A., Gourmelen, N., et al., 2014b. Rapid dynamic activation of a marine-based Arctic ice cap. Geophys. Res. Lett. 41, 8902–8909. https://doi.org/10.1002/2014GL062255.

McMillan, M., Leeson, A., Shepherd, A., et al., 2016. A high-resolution record of Greenland mass balance. Geophys. Res. Lett. 43, 7002–7010. https://doi.org/10.1002/2016GL069666.

Moholdt, G., Nuth, C., Hagen, J.O., Kohler, J., 2010. Recent elevation changes of Svalbard glaciers derived from ICESat laser altimetry. Remote Sens. Environ. 114 (11), 2756–2767. https://doi.org/10.1016/j.rse.2010.06.008.

Nielsen, K., Stenseng, L., Andersen, O.B., Villadsen, H., Knudsen, P., 2015. Validation of CryoSat-2 SAR mode based lake levels, *Remote Sens.* Environ. 171, 162–170. https://doi.org/10.1016/j.rse.2015.10.023.

Pritchard, H.D., Arthern, R.J., Vaughan, D.G., Edwards, L.A., 2009. Extensive dynamic thinning on the margins of the Greenland and Antarctic ice sheets. Nature 461 (7266), 971–975. https://doi.org/10.1038/nature08471.

Raney, K., 1998. The delay/doppler radar altimeter. IEEE Trans. Geosci. Remote Sens. 36 (5), 1578–1588. https://doi.org/10.1109/36.718861.

Remy, F., Mazzega, P., Houry, S., Brossier, C., Minster, J.F., 1989. Mapping of the topography of continental ice by inversion of satellite-altimeter data. J. Glaciol. 35 (119), 98–107. https://doi.org/10.3189/002214389793701419.

Remy, F., Flament, T., Blarel, F., Benveniste, J., 2012. Radar altimetry measurements over antarctic ice sheet: A focus on antenna polarization and change in backscatter problems. Adv. Sp. Res. 50 (8), 998–1006. https://doi.org/10.1016/j.asr.2012.04.003.

Sandwell, D.T., 1987. Biharmonic spline interpolation of GEOS-3 and SEASAT altimeter data. Geophys. Res. Lett. 14 (2), 139–142. https://doi.org/10.1029/GL014i002p00139.

Sandwell, D.T., Müller, R.D., Smith, W.H.F., Garcia, E., Francis, R., (2014), New global marine gravity model from CryoSat-2 and Jason-1 reveals buried tectonic structure., Science 346 (6205), 65–67, doi:10.1126/science.1258213.

Shepherd, A., Wingham, D., Mansley, J., Corr, H., 2001. Inland thinning of Pine Island Glacier West Antarctica. Science 291 (5505), 862–864.

Shepherd, A., Ivins, E.R., A, G.. et al. (2012), A reconciled estimate of ice-sheet mass balance. Science 338 (6111), 1183–1189, doi:10.1126/science.1228102.

Smith, B., Fricker, H.A., Joughin, I., Tulaczyk, S., 2009. An inventory of active subglacial lakes in Antarctica detected by ICESat (2003–2008). J. Glaciol. 55 (192), 573–595.

Sørensen, L.S., Simonsen, S.B., Meister, R., Forsberg, R., Levinsen, J.F., Flament, T., 2015. Envisat-derived elevation changes of the Greenland ice sheet, and a comparison with ICESat results in the accumulation area. Remote Sens Environ. 160, 56–62. https://doi.org/10.1016/j.rse.2014.12.022.

Tilling, R.L., Ridout, A., Shepherd, A., Wingham, D.J., 2015. Increased Arctic sea ice volume after anomalously low melting in 2013. Nat. Geosci. 8 (8), 643–646. https://doi.org/10.1038/ngeo2489.

Vaughan, D.G., Comiso, J.C., Allison, I., 2013. Observations: Cryosphere. In: Stocker, T.F., Qin, D., Plattner, G.-K., Tignor, M., Allen, S.K., Boschung, J., Nauels, A., Xia, Y. (Eds.), Climate Change 2013: Physical Science Basis. Contribution of Working Group I to the Fifth Assessment Report of the Intergovernmental Panel on Climate Change. Cambridge University Press, Cambridge, UK,, pp. 317–382.

Villadsen, H., Andersen, O.B., Stenseng, L., Nielsen, K., Knudsen, P., 2015. CryoSat-2 altimetry for river level monitoring - Evaluation in the Ganges-Brahmaputra River basin. Remote Sens Environ. 168, 80–89. https://doi.org/10.1016/j.rse.2015.05.025.

Wingham, D., Ridout, A., Scharroo, R., Arthern, R., Shum, C., 1998. Antarctic elevation change from 1992 to 1996. Science 282 (5388), 456–458.

Wingham, D., Wallis, D., Shepherd, A., 2009. Spatial and temporal evolution of Pine Island Glacier thinning, 1995–2006. Geophys. Res. Lett. 36, L17501, L17501 10.1029/2009gl039126.

Wingham, D.J., Francis, C.R., Baker, S., et al., 2006a. CryoSat: a mission to determine the fluctuations in Earth's land and marine ice fields. Adv. Space. Res. 37, 841–871.

Wingham, D.J., Shepherd, A., Muir, A., Marshall, G.J., 2006b. Mass balance of the Antarctic ice sheet. Philos. Trans. R. Soc. A-Mathematical Phys Eng. Sci. 364 (1844), 1627–1635. https://doi.org/10.1098/rsta.2006.1792.

Wouters, B., Martin-Espanol, A., Helm, V., Flament, T., van Wessem, J. M., Ligtenberg, S.R.M., van den Broeke, M.R., Bamber, J.L., 2015. Dynamic thinning of glaciers on the Southern Antarctic Peninsula. Science 348 (6237), 899–904.

Zwally, H.J., Giovinetto, M.B., Li, J., Cornejo, H.G., Beckley, M.A., Brenner, A.C., Saba, J.L., Yi, D., 2005. Mass changes of the Greenland and Antarctic ice sheets and shelves and contributions to sea-level rise : 1992–2002. J. Glaciol. 51 (175), 509–527.

Zwally, H.J., Li, J., Brenner, A.C., et al., 2011. Greenland ice sheet mass balance: distribution of increased mass loss with climate warming; 2003–07 versus 1992–2002. J. Glaciol. 57 (201), 88–102. https://doi.org/10.3189/002214311795306682.